Title no. 104-M51

Evaluation of Shrinkage Prediction Models for Self-Consolidating Concrete

by Jaime Fernández-Gómez and Galit Agranati Landsberger

Predicting the shrinkage deformation is an important aspect in the evaluation of the long term behavior of concrete. In this study, experimental shrinkage results for self-consolidating concrete (SCC) and conventional concrete (CC) are compiled from 25 published investigations into a database. The database includes 93 SCC mixtures and 30 CC mixtures. The shrinkage strains for the concrete mixtures are calculated using the following prediction models: CEB-FIP 1990, EHE, ACI 209R, B3, and GL2000. Various analysis methods including best-fit line, residual analysis, and coefficient of variation, are used to compare the predicted and measured shrinkage strains of the SCC and CC mixtures. The influence of various parameters, such as strength of concrete, cement content, filler content, aggregate content, and water-cement ratio (w/c) on the shrinkage behavior of SCC is also included. The ACI 209R and B3 models best estimate the shrinkage strains for SCC and CC. The CEB-FIP 1990, EHE, and GL2000 substantially underestimate the shrinkage strains for both the SCC and CC mixtures. Each of the models, however, predicts the shrinkage strains with similar accuracy for SCC and CC.

Keywords: deformation; self-consolidating concrete; shrinkage models.

INTRODUCTION

Self consolidating concrete (SCC) is a very fluid concrete that can flow through the reinforcement and fill the molds without any need for vibration during the placement process and in the hardened state complies with all the requirements of conventional vibrated concrete (CC). SCC is characterized by its excellent deformability and segregation resistance. SCC basically consists of the same components as conventional vibrated concrete (cement, water, aggregates, admixtures, and mineral additions), but the final composition of the mixture and its fresh characteristics are different. In comparison with conventional concrete, SCC contains larger quantities of mineral fillers such as finely crushed limestone or fly ash, higher quantities of high-range water-reducing admixtures, and the maximum size of the coarse aggregate is smaller.

These modifications in the composition of the mixture affect the behavior of the concrete in its hardened state, including the shrinkage deformations. It is of general acceptance that shrinkage depends mainly on the characteristics of the paste and the aggregate volume. It is considered that concretes with a higher paste volume and a lower aggregate volume exhibit greater shrinkage deformations.[1]

Shrinkage is the volume change caused by the loss of moisture from either fresh or hardened concrete. Shrinkage strains can be classified as plastic, autogenous, drying, or thermal shrinkage. Plastic shrinkage refers to the loss of water from fresh concrete due to surface evaporation. Autogenous shrinkage is caused by the internal consumption of water during the hydration process, resulting in the self-desiccation of the concrete. This phenomenon occurs in concrete with a low water-cement ratio (*w/c*) where there is not enough free water to complete the hydration process. In the case of conventional concrete of moderate resistance, the autogenous shrinkage is small, with values less than 100×10^{-6} m/m, and is usually included together with the drying shrinkage. In the case of high-strength concrete, however, this type of shrinkage can be of importance.[1] Drying shrinkage of the hardened concrete is a more significant phenomenon than the other two described previously. Its magnitude can vary between 300 and 900×10^{-6} m/m. Inadequate provisions for these deformations can lead to excessive cracking of structural elements, which may be unacceptable considering durability criteria.

Various investigations on shrinkage of SCC have been published in the past few years and the conclusions of these are varied. According to Klug,[2] Heirman and Vandewalle,[3] Xie et al.,[4] and Chan et al.,[5] the shrinkage strains of SCC are higher in comparison with CC. Other authors such as Poppe and De Schutter,[6] Bouzoubaa and Lachemi,[7] Vieira and Bettencourt,[8] Assie et al.,[9] and Pons et al.[10] conclude that the shrinkage strains of SCC and CC are equivalent for concretes with similar compression resistance. It should be noted that the differences in experimental results between these investigations can also be due to differences in the concrete mixtures studied, testing conditions, and testing methods.

RESEARCH SIGNIFICANCE

Predicting the shrinkage deformation is an important aspect in the evaluation of the long term behavior of concrete. The actual research on the shrinkage of SCC consists mainly of different studies, each based on limited experimental data, which in many cases lead to contradictory conclusions. To evaluate the overall shrinkage behavior of SCC, a larger number of experimental data is necessary. The main objective of this study is to create an extensive database of SCC shrinkage results that will permit a broader statistical analysis of the results to study the shrinkage behavior of SCC and evaluate the overall applicability of the actual estimating models to SCC.

DATABASE FOR SHRINKAGE TESTS

The use of a database with experimental results from various published investigations is an important tool for studying the applicability of the various shrinkage estimation models to SCC. To apply the estimation models to the particular concrete mixtures, it is necessary to use only investigations that adequately define the applied testing methodology. The

ACI Materials Journal, V. 104, No. 5, September-October 2007.
MS No. M-2006-128.R2 received November 15, 2006, and reviewed under Institute publication policies. Copyright © 2007, American Concrete Institute. All rights reserved, including the making of copies unless permission is obtained from the copyright proprietors. Pertinent discussion including authors' closure, if any, will be published in the July-August 2008 *ACI Materials Journal* if the discussion is received by April 1, 2008.

Jaime Fernández-Gómez *is a Full Professor at the Building and Precasting Department of the Faculty of Civil Engineering, Polytechnic University of Madrid, Madrid, Spain, and Director of the Laboratory of the Instituto Técnico de Materiales y Construcciones (INTEMAC), Spain.*

Galit Agranati Landsberger *is a Doctorate Student at the Building and Precasting Department of the Faculty of Civil Engineering, Polytechnic University of Madrid. She received her BS in civil engineering from Northwestern University, Evanston, IL, and her MSc from the Technion Israel Institute of Technology, Haifa, Israel. Her research interests include deformability properties and durability of concrete.*

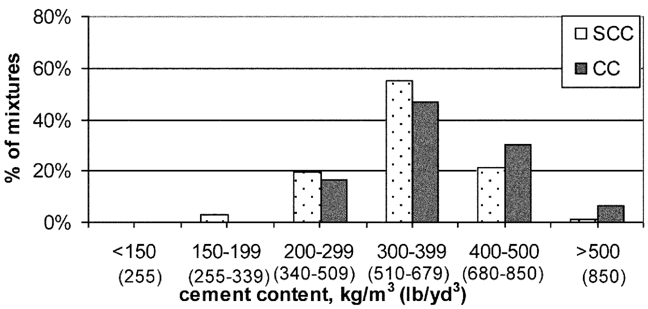

Fig. 1—Cement content distribution of mixtures included in database.

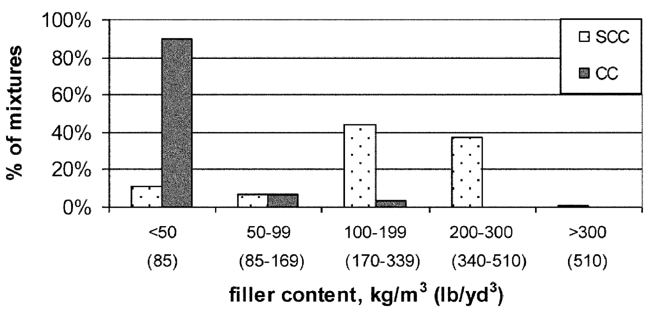

Fig. 2—Filler content distribution of mixtures included in database.

experimental results included in the database proceed mainly from papers presented at various conferences on SCC and from other published articles. The database includes information regarding the composition of the mixtures, fresh properties of SCC, testing methodology and conditions, compression strength, and shrinkage results. It should be emphasized that this aspect has not been researched as extensively as other aspects of SCC, and the published experimental data is still not very extensive.

Using experimental data results from different sources can frequently be problematic for the following reasons:

- There is often insufficient information regarding the exact composition of the concrete mixtures;
- The size of the specimens, curing conditions, and testing methodology vary between the different investigations and, in some cases, this information is not fully indicated;
- In many cases it is difficult to extract the relevant experimental values because the published results are incomplete or are presented in graphical form and the data values have to be extrapolated; and
- Shrinkage tests are time dependant tests of long duration. Parameters such as the age at which shrinkage begins, the total test duration, and the time intervals at which measurements are taken vary between the different investigations.

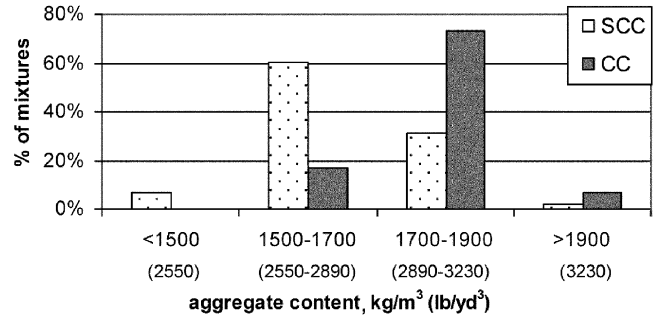

Fig. 3—Aggregate content distribution of mixtures included in database.

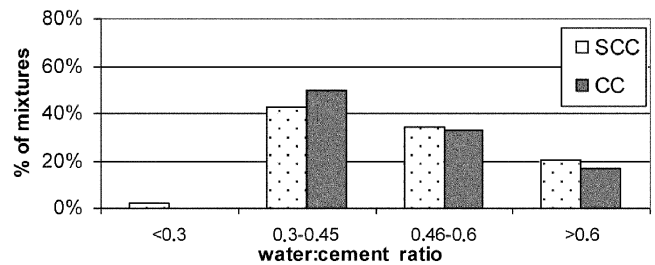

Fig. 4—Water-cement ratio distribution of mixtures included in database.

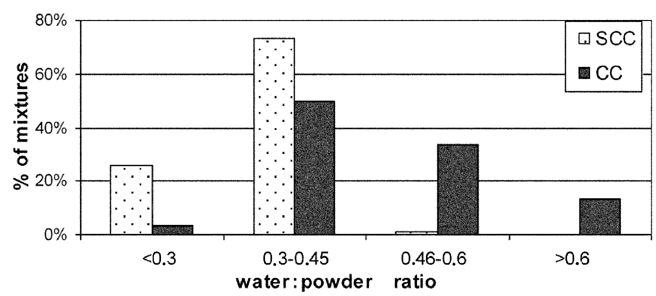

Fig. 5—Water-powder ratio distribution of mixtures included in database.

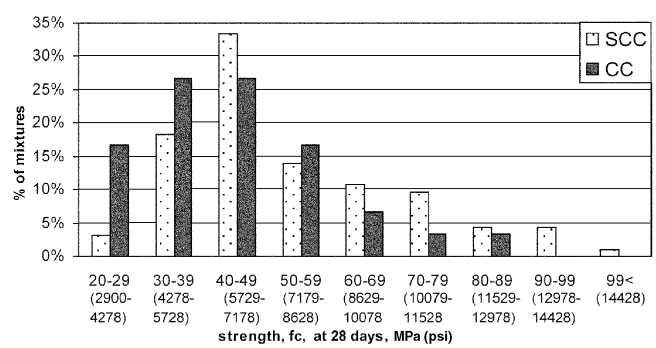

Fig. 6—Twenty-eight-day strength f_c *distribution of mixtures.*

Table 1 is a general summary of the concrete mixtures included in the database. The database includes test results from 25 different investigations, with a total of 123 different concrete mixtures, of which 93 are SCC mixtures and 30 are CC mixtures. Table 1 also includes additional information regarding the age of concrete when drying shrinkage begins, duration of the shrinkage tests, relative humidity, type of specimen, type of cement, and type of mineral addition used.

Table 1—Investigations included in database

	Source	No. of SCC mixtures	No. of CC mixtures	Age of concrete when shrinkage begins, t_s, days	Final age of concrete, days	RH, %	Type of specimen, mm (in.)	Type of cement	Type of filler
1	INTEMAC[11]	2	2	1	90	50	Prism 600 x 150 (23 x 5.9)	CEM II/A-V42.5N	Limestone
2	Heirman and Vandewalle[3]	6	1	1	56	60	Cylinder Ø113 x 300 (4.4 x 11.7)	Not indicated—assume Type I	Limestone, dolomite, fly ash, quartzite
3	Vieira and Betterncourt[8]	1	1	3	180	50	Prism 150 x 150 x 600 (5.9 x 5.9 x 23)	CEM I 42.5R	Limestone, fly ash
4	Proust and Pons [2]	5	2	1	300	55	Cylinder Ø90 x 280 (3.5 x 10.9)	CEM I 52.5 CEM II/A 52.5	Limestone, silica fume
5	Chopin et al.[13]	5	1	1	365	50	Cylinder Ø90 x 280 (3.5 x 10.9)	Not indicated—assume Type I	Limestone
6	Turcry et al.[14]	2	2	1	112	50	Prism 70 x 70 x 280 (2.7 x 2.7 x 10.9)	CEM I 52.5, CEM II 42.5	Limestone
7	Assie et al.[9]	1	1	1	170	50	Cylinder Ø110 x 220 (4.3 x 8.6)	CEM I 52.5 N	Limestone
8	Bouzoubaa and Lachemi[7]	8	1	7	224	50	Prism 76 x 102 x 390 (3 x 4 x 15.2)	ASTM Type I	Fly ash
9	Hans and Pentti[15]	2	2	7	63	50	Prism 100 x 100 x 400 (3 x 3 x 15.6)	OPC I, II	Limestone
10	Poppe and De Schutter[6]	4	0	1	1400	60	Prism 150 x 150 x 500 (5.9 x 5.9 x 19.5)	CEM I 42.5R CEM I 52.5 CEM III A 42.5	Limestone
11	Poppe and De Schutter[16]	2	0	1	300	60	Prism 150 x 150 x 500 (5.9 x 5.9 x 19.5)	CEM I 42.5R	Limestone
12	Xie et al.[4]	5	0	2	90	55	Prism 100 x 100 x 500 (3.9 x 3.9 x 19.5)	CEM I	Fly ash
13	Persson[17]	4	4	1	180	60	Cylinder Ø100 x 500 (3.9 x 19.5)	CEM I CEM II	Glass filler, limestone
14	Persson[18]	3	4	1		60	Cylinder Ø100 x 500 (3.9 x 9.5)	CEM I CEM II	Silica fume, quartzite
15	Suksawang et al.[19]	4	1	1	90	50	Prism 75 x 75 x 285 (2.9 x 2.9 x 11.1)	OPC—assume Type I	Silica fume, fly ash, GGBS
16	Khrapko[20]	3	1	3	56	50	Prism 75 x 75 x 285 (2.9 x 2.9 x 11.1)	CEM I	Fly ash, quarry powder
17	Brunner[21]	15	0	0, 1, 2, 6, 90	360	65	Prism 100 x 100 x 500 (3.9 x 3.9 x 19.5)	CEM II/A-S42.5R	Limestone
18	Song et al.[22]	4	0	1	28	50	Cylinder Ø150 x 300 (5.9 x 11.7)	Not indicate—assume Type I	GGBS
19	See and Attiogbe[23]	4	1	1	160	50	Prism 75 x 75 x 285 (2.9 x 2.9 x 11.1)	Type I/II	Limestone
20	Mørtsell and Rodum[24]	1	1	7	90	50	Prism 100 x 100 x 500 (3.9 x 3.9 x 19.5)	CEM I-52.5LA	Silica fume
21	Persson[25]	4	1	1	500, 300, 28, 20	60	Cylinder Ø100 x 500 (3.9 x 19.5), Ø55 x 500 (2.1 x 19.5)	CEM II/A-D52.5LA	Limestone
22	Rols et al.[26]	1	—	1	90	50	Prism 70 x 70 x 280 (2.7 x 2.7 x 10.9)	CEM I 52.5R	Limestone
23	Chan et al.[27]	1	2	7	90	80	Cylinder Ø100 x 300 (3.9 x 11.7)	Not indicated—assume Type I	Fly ash
24	Sonebi et al.[28]	4	2	7, 1	250	50	Prism 100 x 100 x 400 (3.9 x 3.9 x 15.6) Cylinder 160 x 1000 (6.2 x 39)	CEM 42.5	GGBS, limestone
25	Ozyildrim and Lane[29]	2	0	1	240	50	Prism 75 x 75 x 285 (2.9 x 2.9 x 11.1)	Type II	GGBS
Total of 123 mixtures		93	30						

Note: GGBS = ground granulated blast-furnace slag.

The concrete mixtures vary widely in their composition and characteristics. Figures 1 through 6 show the distribution of the following components and properties of the SCC and CC mixtures: cement content (Fig. 1), filler content (Fig. 2), aggregate content (Fig. 3), *w/c* (Fig. 4), water-powder ratio (*w/p*) (Fig. 5), 28-day strength (Fig. 6), and the slump flow (Fig. 7).

Figure 1 shows the cement content distribution for the mixtures included in the database. The cement content is similar for both types of mixtures, with 55% of the SCC and

47% of the CC mixtures having cement content between 300 and 399 kg/m^3 (510 and 678 lb/yd^3), and 22% of the SCC and 30% of the CC mixtures having cement content between 400 and 500 kg/m^3 (680 and 850 lb/yd^3). The filler content distribution for the SCC mixtures, as shown in Fig. 2, is 44 and 38% with the filler content between 100 and 199 kg/m^3 and 200 and 300 kg/m^3 (170 and 338 kg/m^3 and 340 and 510 lb/yd^3), respectively. In the case of the CC, 90% of the mixtures have a filler content of less than 50 kg/m^3 (85 lb/yd^3).

The aggregate content is one of the main factors affecting the shrinkage strains of concrete. The main function of the aggregate is to restrain the shrinkage deformations. Concretes with a low aggregate content are associated with a higher shrinkage strain. Figure 3 shows the aggregate content for the SCC and CC mixtures included in the database. The aggregate content of SCC is lower than in CC, with 66% of the SCC mixtures and only 17% of the CC mixtures having an aggregate content lower than 1700 kg/m^3 (2890 lb/yd^3). The mean aggregate content is 1666 kg/m^3 (3009 lb/yd^3) for SCC and 1770 kg/m^3 (3009 lb/yd^3) for the CC mixtures.

The *w/c* distribution, shown in Fig. 4, is similar for both types of concretes, with 43 and 50% of the SCC and CC mixtures, respectively, having a *w/c* between 0.3 and 0.45, and 34 and 33% of the SCC and CC, respectively, having a *w/c* between 0.46 and 0.6. The *w/p* distribution, shown in Fig. 5, is very different between the SCC and CC mixtures, with 26% of the SCC mixtures having a *w/p* of less than 0.3, and 73% of the SCC mixtures having a *w/p* between 0.3 and 0.45. Because the CC mixtures have lower filler content, their *w/p* is similar to the *w/c*. The powder content is taken as the sum of the cement and filler content.

The compressive strength of concrete does not directly affect the shrinkage behavior; however, it is an indication of the concrete properties, and most estimating models use it as the main parameter to characterize the concrete. Figure 6 shows the 28-day strength distribution for the mixtures. Considering normal-strength concrete with a 28-day strength between 30 and 60 MPa (4350 and 8700 psi), 65% of the SCC mixtures and a similar percentage of 71% of the CC mixtures are within this range. The percentage of mixtures having a higher strength of 60 MPa (8700 psi) and higher, however, is 30% for SCC and only 13% for CC. It the case of lower strength concrete of 30 MPa (4350 psi) and lower, 3% of the SCC and 17% of the CC mixtures are within this range.

The most common method to characterize the fresh properties of SCC is by its slump flow. Figure 7 shows the slump flow distribution for the SCC mixtures included in the database. It can be observed that 65% of the SCC mixtures have a slump flow between 650 and 800 mm (25.4 and 31.2 in.), and 21% of the SCC mixtures have a lower slump flow between 600 and 649 mm (23.4 and 25.3 in.).

The test duration distribution for the shrinkage tests is shown in Fig. 8. Considering medium test duration as 61 to 200 days, 34% and 53% of the SCC and CC mixtures, respectively, are within this time range. For a longer test duration, between 201 and 500 days, 49% and 37%, of the SCC and CC mixtures, respectively, are within this time range.

SHRINKAGE ESTIMATION MODELS

There are various empirical models for calculating the shrinkage deformation of concrete. These models vary in complexity, precision, and the parameters necessary for the calculations. The estimation models used in this study are the method recommended by the American Concrete Institute (ACI 209R-92),[30] the model of the European Concrete Committee (CEB) (CEB-FIP 1990),[31] and the model adopted by the Spanish Code for Structural Concrete EHE.[32] Other alternative models are the B3 Model developed by Bažant and Baweja[33] and the Gardner and Lockman Model,[34] also known as GL2000. The following is a brief description of these models.

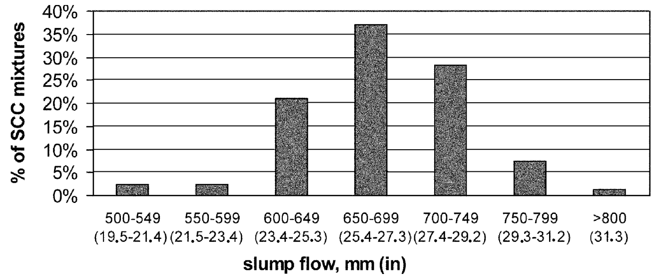

Fig. 7—Slump flow distribution for SCC mixtures.

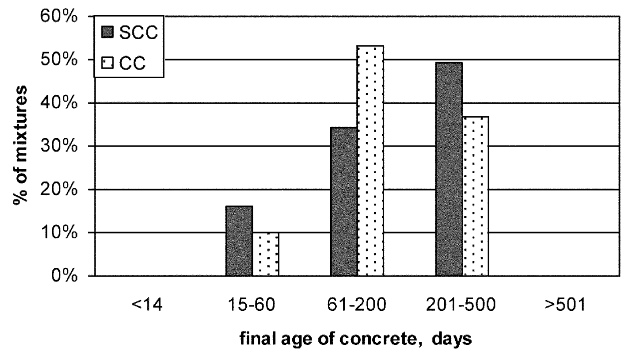

Fig. 8—Final age t *distribution for SCC and CC mixtures.*

ACI 209R-92[30] model

The shrinkage strain $(\varepsilon_{sh})_t$ of concrete at time t after 7 days of moist curing is

$$(\varepsilon_{sh})_t = \frac{t}{35+t}(\varepsilon_{sh})_u \quad (1)$$

The shrinkage strain $(\varepsilon_{sh})_t$ of concrete at time t after 1 to 3 days of steam curing is

$$(\varepsilon_{sh})_t = \frac{t}{55+t}(\varepsilon_{sh})_u \quad (2)$$

where $(\varepsilon_{sh})_u$ is the ultimate shrinkage strain defined as

$$(\varepsilon_{sh})_u = 780\gamma_{sh} \times 10^{-6} \quad (3)$$

where γ_{sh} is the product of the following correction factors: ambient relative humidity γ_λ, initial moist curing γ_{cp}, member size (γ_{vs}, γ_h), concrete composition including slump γ_s, fine aggregate percentage γ_ψ, cement content γ_c, and air content γ_α.

CEB-FIP 1990[31] model

The shrinkage strain ε_{cs} at time t for shrinkage beginning at time t_s is calculated using the following expressions

Table 2—Parameters for calculating shrinkage by different prediction models

Parameters	EHE	CEB-FIP 1990	ACI 209R	B3	GL2000
Relative humidity, %	x	x	x	x	x
Compressive strength at 28 days, f_{c28}	x	x	—	x	x
Specimen size	x	x	x	x	x
Specimen cross section shape (cylinder, cube, prism)	—	—	—	x	—
Time drying starts	x	x	x	x	x
Curing conditions (steam cured, sealed, under water)	—	—	x	x	—
Characteristics of mixture					
Cement content	—	—	x	—	—
Water content	—	—	—	x	—
Fine aggregate content	—	—	x	—	—
Air content	—	—	x	—	—
Cement type	—	x	—	x	x
Slump	—	—	x	—	—

$$\varepsilon_{cs} = \varepsilon_{cs0}\beta_s \quad (4)$$

$$\varepsilon_{cs0} = \varepsilon_s\beta_{RH} \quad (5)$$

$$\varepsilon_s = \left[160 + 10\beta_{sc}\left(9 - \frac{f_{cm}}{10}\right)\right]10^{-6} \quad (6)$$

$$\beta_{RH} = -1.55^*\beta_{sRH} \quad (7)$$

$$\beta_{sRH} = 1 - \left(\frac{RH}{100}\right)^3 \quad (8)$$

$$\beta_s = \sqrt{\frac{(t - t_s)}{350(h/100)^2 + (t - t_s)}} \quad (9)$$

where ε_{cs0} is the basic shrinkage coefficient; β_s is a coefficient that describes the development of shrinkage with time; f_{cm} is the mean compressive strength of the concrete at 28 days; β_{sc} is the correction coefficient for cement type; t is the age of concrete in days; t_s is the age of concrete when shrinkage begins; h is the notional size ($h = 2A_c/u$); A_c is the member cross-sectional area; u is the cross-sectional perimeter; and RH is the relative humidity.

EHE[32] model

The estimation model adopted by the Spanish EHE is based on the CEB-FIP 1990 model. The difference between these two models is that the EHE does not include the coefficient β_{sc}, which accounts for the different cement types. The EHE model uses the compression strength f_{ck} as the only parameter to characterize the concrete. The following expression is used for estimating the shrinkage strain

$$\varepsilon_s = (570 - 5f_{ck})10^{-6} \quad (10)$$

The rest of the expressions included in the EHE model are equivalent to those of the CEB-FIP 1990.

B3[33] model

The shrinkage strain ε_{sh} at time t is defined as

$$\varepsilon_{sh}(t, t_0) = -\varepsilon_{sh\infty}k_hS(t) \quad (11)$$

$$\varepsilon_{s\infty} = -\alpha_1\alpha_2\left\lfloor 1.9\times10^{-2}w^{2.1}f_c^{-0.28} + 270\right\rfloor10^{-6} \quad (12)$$

$$S(t) = \tanh\sqrt{\frac{t - t_0}{\tau_{sh}}} \quad (13)$$

where $\varepsilon_{sh\infty}$ is the ultimate shrinkage, $S(t)$ is the time function for shrinkage; α_1 is the correction term for effect of cement type; α_2 is the correction term for effect of curing conditions; w is the water content; k_h is the humidity dependence factor; t is the age of concrete; t_0 is the age when drying begins; and τ_{sh} is the size dependence factor.

GL2000[34] model

The shrinkage strains ε_{sh} are calculated using the following expressions

$$\varepsilon_{sh} = \varepsilon_{shu}\beta(h)\beta(t) \quad (14)$$

$$\beta(h) = 1 - 1.18h^4 \quad (15)$$

$$\varepsilon_{shu} = 1000K\left(\frac{30}{f_{cm28}}\right)^{1/2}10^{-6} \quad (16)$$

$$\beta(t) = \left(\frac{t - t_c}{t - t_c + 0.15(V/S)^2}\right)^{0.5} \quad (17)$$

where ε_{shu} is the notional ultimate shrinkage strain; $\beta(h)$ is the correction term for effect of humidity; $\beta(t)$ is the correction term for effect of time; h is the relative humidity; t_c is the age of concrete when drying begins in days; t is the age of concrete in days; K is the correction term for effect of cement type; V/S is the volume-surface ratio of the member; and f_{cm28} is the mean compressive strength at 28 days. Table 2 includes a summery of the parameters considered by each of the prediction models for estimating the shrinkage strains.

RESULTS AND ANALYSIS

Comparison between experimental and calculated shrinkage strains

The specific characterization parameters for each concrete mixture are used to calculate the shrinkage strains applying the different estimation models. The experimental and calculated shrinkage strains for the SCC and CC mixtures included in the database are shown in Fig. 9. From Fig. 9(a), it can be observed that the dispersion of the experimental shrinkage values is high in comparison with the various estimating models. This is especially notable for the short term results, up to 90 days, where the dispersion of the experimental results is high, and on the contrary, the calculated strains are much less dispersed. The experimental shrinkage strains for SCC vary between 40 and 1210×10^{-6} m/m with a

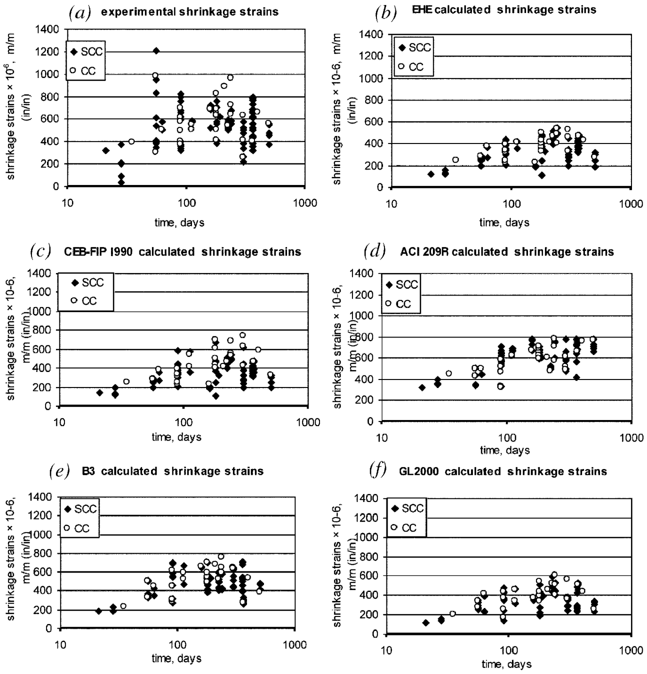

Fig. 9—Shrinkage strains for experimental results and calculated values for various prediction models.

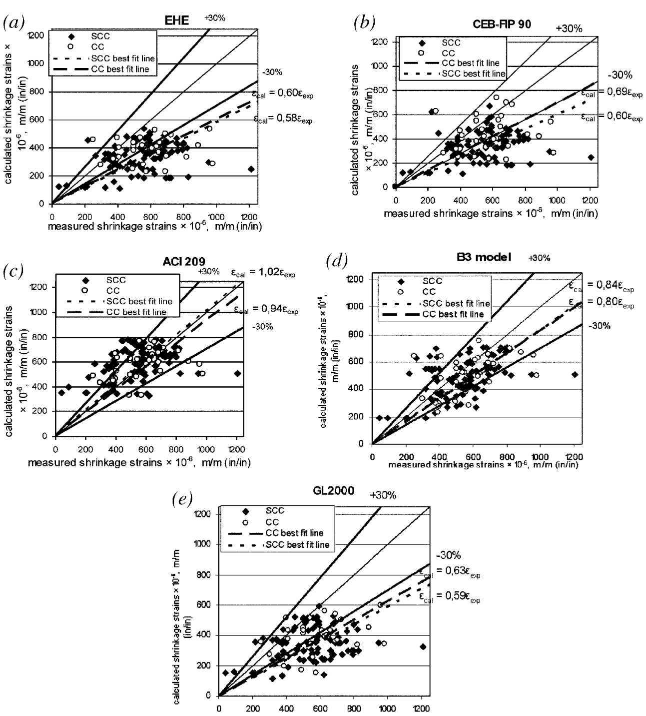

Fig. 10—Comparison between measured and calculated shrinkage strains for various prediction models.

mean value of 540 × 10^{-6} m/m (in./in.), in the case of CC, the strains vary between 253 and 980 × 10^{-6} m/m with a mean value of 581 × 10^{-6} m/m.

Figure 10 includes a comparison between the measured shrinkage values and the calculated values for each of the five estimating models for the SCC and CC mixtures. The figures include, as a reference, the relationship $\varepsilon_{cal} = \varepsilon_{exp}$, which represents the condition of equal values for the calculated and measured shrinkage strains and a target deviation limit of ±30% between the calculated and measured values. Figure 10 also includes the best-fit line, calculated from a linear regression analysis, for the SCC and CC mixtures. A general overview of the results does not indicate a marked difference between the shrinkage behavior of SCC and CC. From Fig. 10(a), (b), and (e), it can be observed that the EHE, CEB-FIP 1990, and the GL2000 models have a general tendency to underestimate the shrinkage values. The ACI 209R model (Fig. 1(c)) has a slight tendency to overestimate the shrinkage results. The shrinkage values calculated using the B3 Model (Fig. 1(d)) seem to fit better within the marked margin of ±30%.

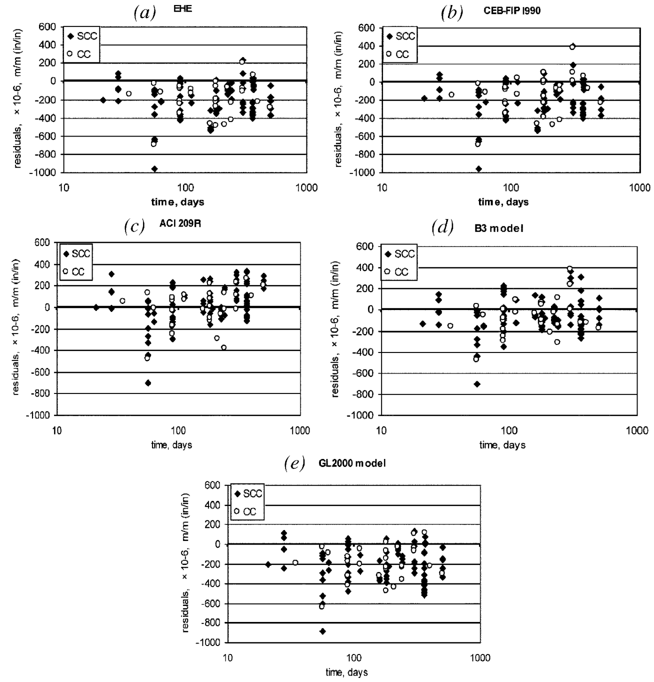

Fig. 11—Residual values for various prediction models.

The best-fit line calculated using a linear regression analysis through zero, shown in Fig. 10, is one of the methods used to analyze the different models. The gradient of the best-fit line and the corresponding correlation coefficients are tabulated in Table 3. The correlation coefficient is an indication of how well the data is grouped about the regression line. The ACI 209R model best estimates the mean shrinkage values with a gradient value of 1.02 and 0.94, for SCC and CC, respectively. The EHE, CEB-FIP 1990, and GL2000 models underestimate the mean shrinkage value for SCC and CC, with a gradient value of approximately 0.60 for both types of concretes. The gradient of the best-fit line using the B3 model slightly underestimates the mean shrinkage values with a gradient value of 0.84 and 0.80 for SCC and CC, respectively. Despite differences between the different models, for each model, there is no significant difference between the best-fit line for SCC and CC.

Residual analysis and coefficient of variation

An alternative method to evaluate the performance of the different estimating models is a residual analysis. The residual value R is defined as the difference between the estimated and the measured shrinkage strains.

$$R = \text{estimated value} - \text{measured value} \tag{18}$$

Table 3—Goodness of fit comparison for different estimation models

	EHE		CEB-FIB 1990		ACI 209R		B3		GL2000	
	Gradient, m	Correlation coefficient	Gradient, m	Correlation coefficient	Gradient, m	Correlation coefficient	Gradient, m	Correlation coefficient	Gradient, m	Correlation coefficient
SCC	0.58	0.87	0.60	0.85	1.02	0.91	0.84	0.91	0.59	0.87
Rating of model*	5		3		1		2		4	
HC	0.60	0.89	0.69	0.85	0.94	0.91	0.80	0.91	0.63	0.90
Rating of model*	5		3		1		2		4	

*Rating of model: 1 = performed best; 5 = performed worst.

The residuals of the SCC and CC mixtures for the different estimation models are plotted in Fig. 11. Positive residuals indicate that the model overestimates the shrinkage strains and negative residuals indicate that the model underestimates them. A model better predicts the shrinkage strains if the residuals are closely centered around the zero axis and if these are equally distributed in the positive and negative ranges. The distributions of the residuals in the negative and positive range for the different models are included in Table 4. It can be observed that for each of the models, the percentage of positive and negative values is similar for both types of concrete. The ACI 209R model shows the best balanced results with a slight overestimation of 66% and 63% of the shrinkage strains for SCC and CC, respectively. The EHE, CEB-FIP 1990, and GL2000 strongly underestimate most of the values. The B3 model also underestimates most of the shrinkage strains, but to a lesser degree.

Another aspect to evaluate is the percentage of residuals that are within a low range of $\pm 150 \times 10^{-6}$ m/m. A prediction model can be considered better if a higher percentage of the residuals are within this low range. Table 4 includes the residuals within the $\pm 150 \times 10^{-6}$ m/m range for both types of concrete and for the different estimating models. The B3 and ACI 209R models perform best with 67% and 59%, respectively, for SCC, and 66% and 67%, respectively, for CC, of the residuals within this marked range. For the GL2000, CEB-FIP 1990, and EHE models, less residuals are included within this range, with values of 45%, 44%, and 43%, respectively, for SCC, and 40%, 57%, and 43%, respectively, for CC.

Table 4 also includes the mean residual, $\Sigma R/n$, for the SCC and CC mixtures. It can be observed that the ACI 209R and B3 models perform best. The ACI 209R model slightly overestimates the residuals, with a mean residual value of 57 and 6×10^{-6} m/m for SCC and CC, respectively. The B3 slightly underestimates the mean residual value, with –60 and -91×10^{-6} m/m for SCC and CC, respectively. The GL2000, CEB-FIP 1990, and EHE models substantially underestimate the mean residual value, with values of –197, –190, and -202×10^{-6} m/m, respectively, for SCC, and –196, –146, and -205×10^{-6} m/m, respectively, for CC.

The residual method is used to indicate the ability of a model to either overestimate or underestimate the shrinkage. It does not necessarily determine, however, which model is the most accurate. To evaluate which model estimates the shrinkage strains with the least error, the coefficient of variation should be compared. The coefficient of variation for the entire drying period for each of the estimating models is calculated using the following equation

Table 4—Results for residual analysis for different estimating models

	EHE	CEB-FIB 1990	ACI 209R	B3	GL2000
Mean residual value, $\times 10^{-6}$ m/m					
SCC	–202	–190	57	–60	–197
CC	–205	–146	6	–91	–196
Distribution of residuals					
SCC					
+ range	10%	11%	66%	27%	14%
– range	90%	89%	34%	73%	86%
CC					
+ range	7%	23%	63%	27%	10%
– range	93%	77%	37%	73%	90%
Residual range inside $\pm 150 \times 10^{-6}$ m/m					
SCC	43%	44%	62%	67%	45%
CC	43%	57%	60%	57%	40%

Table 5—Coefficient of variation of different estimating models

	EHE	CEB-FIB 1990	ACI 209R	B3	GL2000
SCC rating*	0.51 4	0.51 4	0.35 2	0.33 1	0.50 3
CC rating*	0.48 5	0.45 3	0.33 2	0.32 1	0.46 4

*Rating of model: 1 = performed best; 5 = performed worst.

$$w = \frac{1}{\bar{J}}\sqrt{\frac{1}{n-1}\sum_{i=1}^{n} R^2} \quad \bar{J} = \frac{1}{n}\sum_{i=1}^{n} J \tag{19}$$

where w is the variation coefficient; J is the experimental value; R is the residual value; and n is the number of observations.

Table 5 includes the coefficient of variation of the SCC and CC mixtures for the different estimating models. It can bee observed that for each of the estimating the models, the coefficient of variation is similar between SCC and CC. It is also evident that the B3 and ACI 209R models are the most precise in estimating the coefficient of variation, with values of 0.33 and 0.35, respectively, for SCC and 0.32 and 0.33, respectively, for CC. The GL2000, CEB-FIP 1990, and EHE models estimate the shrinkage strains less accurately, with coefficients of variation of 0.50, 0.51, and 0.51, respectively, for SCC and 0.46, 0.45, and 0.48, respectively, for CC.

Influence of various parameters on mean shrinkage strain and coefficient of variation

The influence of various parameters that may affect how the models estimate the shrinkage strains are studied. The parameters considered are concrete strength, cement content,

Table 6—Influence of various parameters on mean shrinkage strains, ×10^{-6} m/m, for each estimating model

Parameters		Experimental results		EHE		CEB-FIP 1990		ACI 209R		B3		GL2000	
		SCC	CC	SCC	CC	SCC	CC	SCC	CC	SCC	CC	SCC	CC
Strength f_c, MPa (psi)	$f_c < 45$ (6525)	558	546	412	401	425	474	612	583	524	494	385	394
	$f_c \geq 45$ (6525)	525	627	285	346	296	385	600	599	448	522	314	373
Cement content c, kg/m^3 (lb/yd^3)	$c \leq 350$ (595)	501	534	382	420	406	503	607	599	445	504	391	426
	$c > 350$ (595)	563	618	307	344	311	384	603	583	501	508	311	353
Filler content f, kg/m^3 (lb/yd^3)	$f < 200$ (340)	517	581	323	377	342	435	612	590	475	506	355	385
	$f \geq 200$ (340)	533	*	345	*	345	*	578	*	464	*	314	*
Aggregate content a, kg/m^3 (lb/yd^3)	$a \leq 1700$	545	702	348	412	360	497	607	673	478	611	343	411
	$a > 1700$	525	545	314	366	327	416	599	565	481	474	344	377
Water/cement ratio, w/c	$w/c < 0{,}5$	538	618	294	344	299	384	628	583	462	508	326	353
	$w/c \geq 0{,}5$	539	534	375	420	394	503	583	599	494	504	358	426
Water/powder ratio, w/p	$w/p < 0{,}35$	462	565	291	396	298	483	587	721	393	488	299	400
	$w/p \geq 0{,}35$	519	611	374	319	390	319	604	574	508	508	402	284

*None of CC mixtures contain filler content ≥ 200 kg/m^3 (340 lb/yd^3).

Table 7—Influence of various parameters on gradient *m* of best-fit line for each estimating model

		EHE		CEB-FIP 1990		ACI 209R		B3		GL2000	
		SCC	CC	SCC	CC	SCC	CC	SCC	CC	SCC	CC
Strength f_c, MPa (psi)	$f_c < 45$ (6525)	0.69	0.90	0.71	0.83	1.04	1.00	0.90	0.86	0.64	0.70
	$f_c \geq 45$ (6525)	0.49	0.50	0.51	0.56	1.03	0.88	0.79	0.80	0.55	0.55
Cement content c, kg/m^3 (lb/yd^3)	$c \leq 350$ (595)	0.73	0.73	0.78	0.88	1.14	1.03	0.85	0.88	0.75	0.76
	$c > 350$ (595)	0.50	0.52	0.50	0.58	0.98	1.36	0.83	1.03	0.51	0.54
Filler content f, kg/m^3 (lb/yd^3)	$f < 200$ (340)	0.56	0.60	0.59	0.69	1.06	0.94	0.85	0.83	0.62	0.63
	$f \geq 200$ (340)	0.62	*	0.62	*	1.02	*	0.84	*	0.55	*
Aggregate content a, kg/m^3 (lb/yd^3)	$a \leq 1700$	0.59	0.57	0.61	0.69	1.04	0.93	0.82	0.86	0.58	0.57
	$a > 1700$	0.55	0.61	0.56	0.70	1.03	0.95	0.86	0.82	0.61	0.65
Water/cement ratio, w/c	$w/c < 0.5$	0.48	0.52	0.49	0.58	1.05	0.89	0.79	0.80	0.55	0.54
	$w/c \geq 0.5$	0.66	0.73	0.69	0.88	1.02	1.03	0.88	0.88	0.63	0.76
Water/powder ratio, w/p	$w/p < 0.35$	0.55	0.67	0.57	0.84	1.13	1.24	0.76	0.88	0.57	0.67
	$w/p \geq 0.35$	0.70	0.47	0.73	0.47	1.12	0.84	0.94	0.76	0.75	0.42

*None of CC mixtures contain filler content ≥ 200 kg/m^3 (340 lb/yd^3).

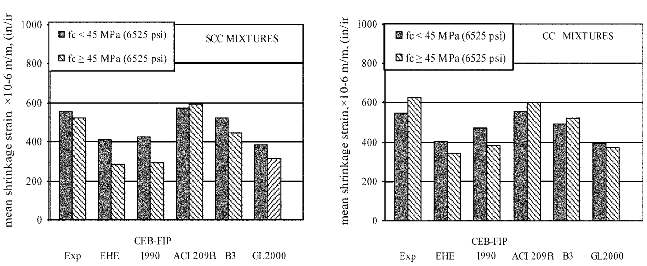

Fig. 12—Mean shrinkage strains for SCC and CC mixtures with f_c *< 45 MPa (6525 psi) and* f_c *≥ 45 MPa (6525 psi).*

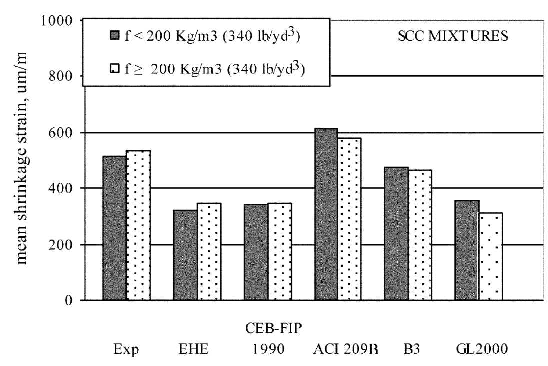

Fig. 13—Mean shrinkage strains for SCC mixtures with filler content f *< 200 kg/m^3 (340 lb/yd^3) and* f *≥ 200 kg/m^3 (340 lb/yd^3).*

filler content, aggregate content, *w/c*, and water-filler ratio. It should be mentioned that the EHE, CEB-FIP 1990, and GL2000 models use the concrete strength f_c as the main concrete characteristic for calculating the shrinkage strains. The B3 model considers the concrete strength f_c together with the water content, and the ACI 209R model uses the fine aggregate percentage, cement content, and air content for characterizing the concrete in their estimating models.

The influence of these parameters is studied on the mean shrinkage strain, best-fit line, and coefficient of variation. Table 6 shows the mean shrinkage strains for the specific conditions analyzed for each of the five parameters. From Fig. 12 it can be observed that the mean shrinkage strain calculated using the ACI 209R model is equivalent to the measured mean shrinkage strains for the SCC and CC mixtures for both strength ranges considered, $f_c < 45$ MPa (6525 psi) and $f_c < 45$ MPa (6525 psi). The EHE, CEB-FIB 1990, and GL2000 models underestimate the mean

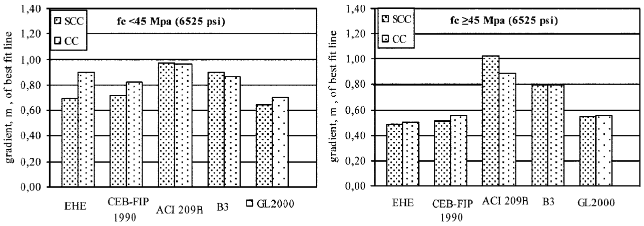

Fig. 14—Gradient m *of best-fit line for SCC and CC mixtures with* f_c *< 45 MPa (6525 psi) and* f_c *≥ 45 MPa (6525 psi).*

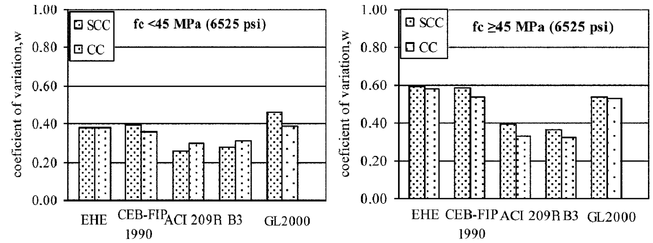

Fig. 15—Coefficient of variation w *for SCC and CC mixtures with* f_c *< 45 MPa (6525 psi) and* f_c *≥ 45 MPa (6525 psi).*

Table 8—Influence of various factors on coefficient of variation for each estimating model

		EHE		CEB-FIP 1990		ACI 209R		B3		GL2000	
		SCC	CC	SCC	CC	SCC	CC	SCC	CC	SCC	CC
Strength f_c, MPa (psi)	f_c < 45 (6525)	0.38	0.38	0.39	0.36	0.28	0.31	0.28	0.31	0.46	0.39
	f_c ≥ 45 (6525)	0.59	0.58	0.58	0.54	0.40	0.35	0.37	0.33	0.54	0.53
Cement content c, kg/m³ (lb/yd³)	c ≤ 350 (595)	0.35	0.36	0.34	0.34	0.36	0.32	0.30	0.31	0.30	0.31
	c > 350 (595)	0.58	0.55	0.58	0.51	0.34	0.34	0.35	0.33	0.56	0.53
Filler content f, kg/m³ (lb/yd³)	f < 200 (340)	0.56	0.48	0.55	0.45	0.41	0.33	0.36	0.32	0.48	0.46
	f ≥ 200 (340)	0.44	*	0.44	*	0.29	*	0.28	*	0.54	*
Aggregate content a, kg/m³ (lb/yd³)	a ≤ 1700	0.48	0.49	0.48	0.40	0.35	0.24	0.34	0.21	0.51	0.48
	a >1700	0.57	0.49	0.57	0.49	0.37	0.37	0.32	0.36	0.49	0.46
Water/cement ratio, w/c	w/c < 0.5	0.61	0.55	0.61	0.51	0.42	0.34	0.39	0.33	0.55	0.53
	w/c ≥ 0.5	0.40	0.36	0.40	0.34	0.28	0.32	0.27	0.31	0.46	0.31
Water/powder ratio, w/p	w/p < 0.35	0.57	0.45	0.57	0.27	0.50	0.37	0.41	0.28	0.55	0.47
	w/p ≥ 0.35	0.36	0.63	0.34	0.63	0.28	0.35	0.27	0.38	0.34	0.66

*None of CC mixtures contain filler content ≥ 200 kg/m³ (340 lb/yd³).

shrinkage strains for both strength ranges and for both types of concretes. The B3 model slightly underestimates the mean shrinkage strains. It can also be observed that the measured mean shrinkage strains for SCC and CC do not vary significantly between the two strength ranges. Figure 13 compares the mean shrinkage results for the SCC mixtures with a filler content f of less than 200 kg/m³ (340 lb/yd³) and ≥200 kg/m³ (340 lb/yd³). It can be observed than the measured mean shrinkage strain does not vary between mixtures with high or low filler content.

Table 7 includes the gradient of the best-fit line m for each of the estimating models and the five chosen parameters. Comparing the concrete resistance f_c, it can be observed in Fig. 14 that the ACI 209R and B3 models behave similarly for both conditions, f_c < 45 MPa (6525 psi) and f_c ≥ 45 MPa (6525 psi); however, the rest of the models behave better for the condition f_c < 45 MPa (6525 psi). This difference is even more pronounced when comparing the conditions c ≤ 350 kg/m³ (595 lb/yd³) and c > 350 kg/m³ (595 lb/yd³).

Table 8 includes the coefficient of variation of each of the estimating models for the five chosen parameters. It can be observed that for the five parameters, the general tendency is similar when compared with the coefficient of variation for the entire database (Table 5). In general, the ACI 209R and the B3 models have lower coefficient of variation than the EHE, CEB-FIP 1990, and GL2000 models. For each model and condition, the coefficient of variation is, generally, similar for both types of concretes. From Fig. 15, it can be observed that for lower strength concretes, f_c < 45 MPa (6525 psi), the coefficient of variation is lower for the SCC and CC mixtures in comparison with f_c ≥ 45 MPa (6525 psi).

CONCLUSIONS

This study presents an extensive database of shrinkage results for SCC and evaluates five shrinkage estimating models and their applicability to this type of concrete. The models considered are the CEB-FIP 1990, EHE, ACI 209R, B3, and GL2000 models. Even though a more extensive database with longer test durations would be advisable, nevertheless, there is a clear behavior pattern in the information that permits the following conclusions to be established:

1. Despite differences between the different models, for each model, there is no significant difference in the shrinkage strain estimation for SCC and CC. Each of the five estimating models (CEB-FIP 1990, EHE, ACI 209R, B3, and GL2000) predict the shrinkage strains with similar precision for both types of concrete—SCC and CC;

2. Considering three statistical methods (best-fit line, residual analysis, and coefficient of variation), it is evident that the B3 and the ACI 209R models are the best models to estimate shrinkage deformations of SCC and CC;

3. The B3 model slightly underestimates the shrinkage strains for SCC and CC; however, the coefficients of variation of this model are the lowest, together with the ACI 209R model. According to the residual analysis, the ACI 209R model slightly overestimates the shrinkage values for SCC and CC. The CEB-FIP 1990, EHE, and GL2000 models substantially underestimate the shrinkage strains for SCC and CC; and

4. Comparing the shrinkage strains of concretes with f_c ≤ 45 MPa (6525 psi) and f_c > 45 MPa (6525 psi), it can be observed that the CEB-FIP 1990, EHE, and GL2000 models estimate the shrinkage strains better for SCC and CC mixtures with strength f_c ≤ 45 MPa (6525 psi). The ACI 209R and B3 models estimate the shrinkage strains with similar precision for both strength ranges.

REFERENCES

1. Neville, A. M., *Properties of Concrete*, 4th Edition, Pearson Education Limited, Harlow, UK, 1996, 844 pp.

2. Klug, Y., and Holschemacher, K., "Comparison of the Hardened Properties of Self Compacting and Normal Vibrated Concrete," *RILEM Proceedings PRO* 33, 2003, pp. 596-605.

3. Heirman, G., and Vandewalle, L., "The Influence of Fillers on the Properties of Self Compacting Concrete in Fresh and Hardened State," *RILEM Proceedings PRO* 33, 2003, pp. 606-618.

4. Xie, Y.; Li, Y.; and Long, G., "Influence of Aggregate on Properties of Self Consolidating Concrete," *RILEM Proceedings PRO* 42, 2005, pp. 161-171.

5. Chan, Y. W.; Chern, J. C.; Hong, C. Y.; and Lue, J. W., "The Analysis of Shrinkage Behavior of SCC and OPC under Various Weather Conditions," *RILEM Proceedings PRO* 17, 2004, pp. 493-506.

6. Poppe, A., and De Schutter, G., "Creep and Shrinkage of Self Compacting Concrete," *RILEM Proceedings PRO* 42, 2005, pp. 329-336.

7. Bouzoubaa, N., and Lachemi, M., "Self-Compacting Concrete Incorporating High Volumes of Class F Fly Ash," *Cement Concrete*, V. 31, 2001, pp. 413-442.

8. Vieira, M., and Bettencourt, A., "Deformability of Hardened SCC," *RILEM Proceedings PRO* 33, 2003, pp. 606-618.

9. Assie, S.; Escadeillas, G.; and Marchese, G., "Durability of Self Compacting Concrete," *RILEM Proceedings PRO* 33, 2003, pp. 655-662.

10. Pons, G.; Proust, E.; and Assie, S., "Creep and Shrinkage of Self Compacting Concrete: A Different Behaviour Compared with Vibrated Concrete?" *RILEM Proceedings PRO* 33, 2003, pp. 645-654.

11. INTEMAC, "Informe Sobre la Investigación Desarrollada para Comparar las Propiedades Mecánicas de los Hormigones Convencionales y Autocompactantes," Document No. TI/LC-05003, 2005, 84 pp.

12. Proust, E., and Pons, G., "Macroscopic and Microscopic Behavior of Self Compacting Concrete Creep and Shrinkage," *Creep Shrinkage and Durability Mechanics of Concrete and Other Quasi-Brittle Materials*, F. J. Ulm, Z. P. Bažant, and W. H. Whittman, eds., Elsevier, 2001, pp. 569-574.

13. Chopin, D.; Francy, O.; Lebourgeois, S.; and Rougeau, P., "Creep and Shrinkage of Heat-Cured Self-Compacting Concrete (SCC)," *RILEM Proceedings PRO* 33, 2003, pp. 672-683.

14. Turcry, F.; Loukili, A.; and Haider, K., "Mechanical Properties, Plastic Shrinkage, and Free Deformation of Self-Consolidating Concrete," *Proceedings of the First North American Conference on the Design and Use of Self-Consolidation Concrete*, 2003, pp. 152-158.

15. Hans, E. G., and Pentti, P., "Properties of SCC—Especially Early Age and Long Term Shrinkage and Salt Frost Resistance," *RILEM Proceedings PRO* 7, 1999, pp. 211-225.

16. Poppe, A. M., and De Schutter, G., "Creep and Shrinkage of Self-Compacting Concrete," *Creep Shrinkage and Durability Mechanics of Concrete and other Quasi-Brittle Materials*, F. J. Ulm, Z. P. Bažant, and W. H. Whittman, eds., Elsevier, 2001, pp. 563-568.

17. Persson, B., "Shrinkage and Strength of Self-Compacting Concrete with Different Kinds of Filler," *RILEM Proceedings PRO* 17, 2004, pp. 191-214.

18. Persson, B., "Creep, Shrinkage and Elastic Modulus of Self-Compacting Concrete," *RILEM Proceedings PRO* 7, 1999, pp. 239-250.

19. Suksawang, N.; Nassif, H. F.; and Najm, H. S., "Durability of Self-Compacting Concrete (SCC) with Pozzolanic Materials," *Proceedings of the First North American Conference on the Design and Use of Self-Consolidation Concrete*, 2003, pp. 305-310, pp. 305-310.

20. Khrapko, M., "Development of SCC Containing Quarry Rock Dust," *Proceedings of the First North American Conference on the Design and Use of Self-Consolidation Concrete*, 2003, pp. 203-209.

21. Brunner, M., "Durability of SCC with High Water Content," *Proceedings of the First North American Conference on the Design and Use of Self-Consolidation Concrete*, 2003, pp. 333-339.

22. Song, H. W.; Byun K. J.; Kim, S. H.; and Choi, D. H., "Early Creep and Shrinkage in Self Compacting Concrete Incorporating GGBFS," *Proceeding of the Second International Symposium on Self-Compacting Concrete*, 2001, pp. 413-421.

23. See, H. T., and Attiogbe, E. K., "Performance of Self-Consolidating Concrete under Restrained Shrinkage," *Shrinkage and Creep of Concrete*, SP-227, N. J. Gardner and J. Weiss, eds., American Concrete Institute, Farmington Hills, MI, 2005, pp. 303-315.

24. Mørtell, E., and Rodum, E., "Mechanical and Durability Aspects of SCC for Road Structures," *Proceeding of the Second International Symposium on Self-Compacting Concrete*, 2001, pp. 459-467.

25. Persson, B., "Shrinkage and Creep of High Performance Self-Compacting Concrete (HPSCC)," *Autogenous Deformation of Concrete*, SP-220, O. M. Jensen, D. P. Bentz, and P. Lura, eds., American Concrete Institute, Farmington Hills, MI, 2005, pp. 155-179.

26. Rols, S.; Ambroise, J.; and Pera, J., "Effect of Different Viscosity Agents on the Properties of Self-Leveling Concrete," *Cement and Concrete Research*, No. 29, 1999, pp. 261-266.

27. Chan, Y. W.; Chern, J. C.; Hong, C. Y.; and Lue, J. W., "The Analysis of Shrinkage Behavior of SCC and OPC under Various Weather Conditions," *RILEM Proceedings PRO* 17 Shrinkage, 2000, pp. 493-506.

28. Sonebi, M.; Bartos, P. J. M.; Zhu, W.; Gibas, J.; and Tamimi, A., "Brite EuRam Project BRPR-CT96-0366," Task 4—Properties of Hardened SCC Concrete, 2000, pp. 6-23.

29. Ozyildririm, C., and Lane, S. D., "Evaluation of Self-Consolidating Concrete—Final Report," CTRC 03-13, Viriginia Transportation Research Council, 2003, pp. 1-15.

30. ACI Committee 209, "Prediction of Creep, Shrinkage, and Temperature Effects in Concrete Structures (ACI 209R-92)," American Concrete Institute, Farmington Hills, MI, 1992, 47 pp.

31. CEB-FIP 1990, "Model Code for Concrete Structures," *Bulletin d'Information*, No. 199, 1991, 201 pp.

32. EHE, "Instrucción de Hormigón Estructural," *Comisión Permanente del Hormigón*, 5th Edición, Madrid, Ministerio de Fomento, 2002, 476 pp.

33. Bažant, Z. P., "Creep and Shrinkage Prediction Models for Analysis and Design of Concrete Structures—Model B3," *Materials and Structures*, V. 28, 1995, pp. 357-365.

34. Gardner, N. J., and Lockman, M. J., "Design Provisions for Drying Shrinkage and Creep of Normal-Strength Concrete," *ACI Materials Journal*, V. 98, No. 2, Mar.-Apr. 2001, pp. 159-167.

Reproduced with permission of the copyright owner. Further reproduction prohibited without permission.